A Generalized Compressible Reynolds Lubrication Equation with Bounded Contact Pressure

Lin Wu and D. B. Bogy

Computer Mechanics Laboratory, Department of Mechanical Engineering

University of California at Berkeley, Berkeley, CA 94720

ABSTRACT

A new modified Reynolds equation is derived based on physical principles for rarefied gas for compressible and extremely thin layer gas lubrication. For the one dimensional problem, theoretical analysis and numerical simulation are employed to show that the new equation does not predict an unphysical unbounded pressure singularity in the limit of contact between the bearing surface and the moving surface. We also show the same is true for other existing models with higher than first order slippage correction, which introduce additional diffusion terms that are functions of the spacing with similar order to that of the convection terms. These developments remove the ambiguity of some previously published analyses and corrects prior erroneous statements that all existing generalized Reynolds equation models predict nonintegrable singular pressure fields in the limit of contact. The asymptotic analysis also supplies a means for deriving the needed additional boundary condition at the boundary of a contact region. For the two dimensional problem, we show by numerical analysis that there are also no unbounded contact pressure singularities for the new model and other models with corrections higher than first order, and that the singularity is weaker than in the 1-D case for these lower order correction models due to the cross diffusion effect introduced by the additional dimension.

I. INTRODUCTION

In gas lubrication bearings contact between the bearing surface and the moving surface is unavoidable under certain situations. The contact gas bearing pressure plays an important role in the dynamic response of bearing systems with intermittent contact. In modern hard disk drives, the read-write head flies above the disk where magnetic information is stored at a height generally less than 50 nm. The extremely thin air bearing between the slider (head) and rotating disk provides the necessary equilibrating lifting force, so the head can fly at the desired height. To increase the areal density further, to the range of 1 Tbit/in^2 , a flying height around 3nm is believed to be necessary. The peak-to-peak roughness of the disk surface is unavoidable and may be about 10-20 nanometers. As a result, intermittent contact between the slider and the disk could be a frequent phenomenon. To predict the bearing pressure accurately, even when actual contact occurs, becomes extremely important in the design of the components of the hard disk drive and other near contact gas lubrication systems.

At these low flying heights, which are only a fraction of the gas molecular mean free path, the traditional macroscopic Reynolds equation based on the continuum assumption with non-slip boundary conditions is no longer valid. Two approaches to modify the Reynolds equation, taking into account the slippage at the boundaries and rarefication effects, have been presented in the literature. The first order slip model of Burgdorfer,[1] the second order slip model of Hsia and Domoto[2] and the 1.5 order slip model of Mitsuya[3] fall under the first approach, which incorporates different order slippage boundary conditions into the integration of the traditional macroscopic continuum compressible Stokes equation under the isothermal assumption. The FK

model of Fukui and Kaneko[4] is an example of the second approach, which uses the linearized Boltzmann equation with slip boundary conditions.

There has been a widely accepted view that all of the above models predict unbounded nonintegrable, singular pressure fields at contact points.[5,6,7] Although Anaya-Dufresne and Sinclair's three term simple polynomial expansion analysis did show there is a possibility that the lowest order term is non-singular at the contact point,[5] their purpose was to find the orders of possible singularity solutions in simple polynomial form, but their analysis could not determine if contact pressure singularities actually occur. In a related problem Anaya-Dufresne[8] successfully removed the contact singularity in the incompressible Taylor plate scraping problem by introducing additional slippage into Maxwell's slip boundary condition through a momentum balance inside the Knudsen layer where the molecules collide or bounce back from collision with the solid wall. He derived a new incompressible Reynolds equation using the new slip boundary condition, and he showed that the equation does not predict a contact pressure singularity. He also numerically showed that the incompressible second and 1.5 order slip models do not have contact pressure singularities. He also assumed that the same conclusions would hold for the compressible case even though he did no further analysis. Here we extend his approach to derive a slip boundary condition at the gas-solid boundary for the compressible case, which is found to be essentially the same as that of the incompressible case.[8] Therefore, to a first order approximation, compressibility can be ignored in this derivation. Also a 2-dimensional modified Reynolds equation is derived by incorporating the modified slip boundary condition into the Stokes equation. The resulting equation has

a form similar to that of the second order and the 1.5 order correction models, differing only by the coefficients in the diffusion terms.

Analytical solutions are derived near the contact point for a 1-dimensional parabolic asperity contact problem, using the first order and second order slip models after simplification of the governing equations by dimensional analysis. Numerical solutions of the full equations are also obtained by a finite volume scheme. The theoretical and numerical solutions are found to be in excellent agreement, and they show there is no unbounded pressure singularity at the contact point for second order type models. This is contradictory to previous analysis and asertion.[5,6,7] As the minimum spacing is reduced to near contact, a narrow boundary layer appears near the contact point within which the pressure quickly drops from the upwind positive value to a sub-ambient value downwind of the point. A shock wave like bounded discontinuity appears when actual contact occurs, which is consistent with the fact that the upwind and downwind transfer of information is blocked by the contact. This spacing reduction limiting process suggests a way to supply the additional boundary condition needed at the contact edge to solve the problem in which gas is funneled into a converging corner or expands from a diverging corner. Since the Reynolds equation is second order it needs two boundary conditions. In the far field ($X = \pm 1$), ambient pressure is assumed as one boundary condition, but it is somewhat difficult to envision the appropriate boundary condition at the contact edge. The asymptotic values obtained from another problem with symmetrical geometry immediately before or after the discontinuity can be used as the boundary condition at the contact point for the converging corner or the diverging corner problem.

It is then shown that unbounded pressure fields are predicted by the first order slip model and the FK model near the contact region. This happens because the order of the diffusion terms expressed as functions of the spacing parameter of the first order slip model and the FK model are higher than these of the convection terms, so the convection effect has no balancing diffusion counter part. Thus the unbounded and nonintegrable pressure singularity is unavoidable in these cases. The singularity in the first order slip model is stronger than that of the FK model, due to the fact that the diffusion term of the first order slip model is asymptotically smaller than in the FK model. We conclude from this asymptotic analysis that removal of the contact singularity, which is viewed as non-physical, requires the diffusion term to scale to the same order in the spacing as the convection term.

For the two dimensional problem in which the 1-D parabolic asperity is rotated about its symmetry axes, similar conclusions can be reached by numerical calculation. The only difference is that the pressure profile is smoother and without the discontinuity for the higher order correction models and the singularity is weaker for models that have a contact singularity.

II. THE DERIVATION OF A MODIFIED REYNOLDS EQUATION WITH BOUNDED CONTACT PRESSURE

For low Reynolds number steady state flow, the governing equation is the Stokes equation. After taking into account the small slope and much smaller spacing in the bearing thickness direction than the length scales in the horizontal directions, one obtains the following lubrication equations

$$0 = -\frac{\partial p}{\partial x} + \mu \frac{\partial^2 u}{\partial z^2},$$

$$0 = -\frac{\partial p}{\partial y} + \mu \frac{\partial^2 v}{\partial z^2},$$

$$\frac{\partial p}{\partial z} = 0, \tag{1}$$

where p is the pressure, μ is the dynamic viscosity of the gas, u and v are gas velocities in the x and y directions, respectively. The above equations can be integrated in the z direction to give the velocity distribution. But two boundary conditions are needed, one at the upper and one at the lower gas-solid interfaces.

The Maxwell slip velocity at the gas-solid interface is derived by equating the momentum transfer rate from the gas molecules to the solid wall through collisions to the macroscopic shear stress of the gas at the solid wall,[9]

$$u_{slip} = \frac{2-\alpha}{\alpha} \lambda \left. \frac{\partial u}{\partial z} \right|_{z=0} = a\lambda \left. \frac{\partial u}{\partial z} \right|_{z=0}, \tag{2}$$

where α is the accommodation coefficent representing the portion of the molecules inside the Knudsen layer that collide with the wall, which usually is taken to be 1. a is the surface correction coefficient. In solving Taylor's incompressible plate scraping problem, Anaya-Dufresne[8] argues that when the scraper is vertical, $u = 0$ along the scraper and so $\frac{\partial u}{\partial z} = 0$ at the contact point, so eq. (2) gives zero slip velocity there where a maximum slip velocity, which reduces the mean velocity to zero, is required physically. As a result, he used momentum balance along the wall direction inside the Knudsen layer, so the normal stress gradient in the direction of the moving plate also forces some

slippage. Here we extend his idea to derive a compressible slip boundary condition. By using a control volume with a length $\Delta x, \Delta y$ and $\Delta z = \lambda$ in the x, y and z directions, respectively (see figure 1), ignoring higher order terms, and applying the x momentum balance we obtain

$$\tau_{x0} = \mu \frac{\partial u}{\partial z}\bigg|_{z=\lambda} + \lambda \frac{\partial \sigma_x}{\partial x}\bigg|_{z=\frac{1}{2}\lambda}, \tag{3}$$

where

$$\tau_{x0} = \frac{\rho \bar{c} \alpha u_{slip}}{2(2-\alpha)}$$

is the momentum transfer rate from the gas molecules to the solid wall.[9] $\bar{c}$ is the average molecular speed, u_{slip} is the slip velocity in the x direction. σ_x is the normal stress

$$\sigma_x = -p - \frac{2}{3}\mu div\underline{u} + 2\mu \frac{\partial u}{\partial x}. \tag{4}$$

Just as in the derivations of the first and second order slip boundary conditions, the length of the control volume in the direction normal to the wall is assumed to be the mean free path. Since λ is a small number in the order of 10^{-8} and ignoring higher order effects, we can evaluate the terms on the right hand side of eq. (3) at $z = 0$ instead of at $z = \lambda$ and $z = \lambda/2$, respectively. Substituting eq. (4) into eq. (3) and using the relationship[9]

$$\mu = \frac{1}{2}\rho \bar{c} \lambda$$

while keeping terms of order $O(\lambda)$, we obtain for the slip velocity in the x direction

$$u_{slip} = \frac{(2-\alpha)}{\alpha}\left(\lambda \frac{\partial u}{\partial z} - \frac{2\lambda}{\rho \bar{c}} \frac{\partial p}{\partial x} \right), \tag{5a}$$

which is exactly the same as that derived by Anaya-Dufresne[8] for an incompressible gas. Therefore compressibility introduces only higher order effects that can be ignored in the first order approximation. Similarly, we can derive the slip velocity in the y direction

$$v_{slip} = \frac{(2-\alpha)}{\alpha}\left(\lambda\frac{\partial v}{\partial z} - \frac{2\lambda}{\rho\bar{c}}\frac{\partial p}{\partial y}\right). \tag{5b}$$

The velocity components u and v can be obtained as functions of z after integrating eq. (1) and applying equations (5a) and (5b) at the upper and lower solid surfaces. The compressible Reynolds equation then follows from substituting the velocities into and integrating the continuity equation. After using the assumptions that the gas is ideal and the gas layer is isothermal, we obtain

$$\begin{aligned}&\frac{\partial}{\partial X}\left[\left(PH^3 + \beta K_n H^2 + \gamma K_n^2\frac{H}{P}\right)\frac{\partial P}{\partial X}\right] + \frac{\partial}{\partial Y}\left[\left(PH^3 + \beta K_n H^2 + \gamma K_n^2\frac{H}{P}\right)\frac{\partial P}{\partial Y}\right] \\ &= \Lambda_x\frac{\partial}{\partial X}(PH) + \Lambda_y\frac{\partial}{\partial Y}(PH)\end{aligned} \tag{6}$$

In the above equation, P and H are the dimesionless pressure and spacing between the upper and lower surfaces, normalized by the ambient pressure p_a and the smallest spacing h_0, respectively. $\Lambda_x = 6\mu UL/p_a h_0^2$ and $\Lambda_y = 6\mu VL/p_a h_0^2$ are the bearing numbers in the x and y directions, respectively, which represent the relative importance between the convection effect and the diffusion effect. L is the horizontal length scale. X and Y are dimensionless coordinates normalized by L. β and γ are two model constants, which for the current derivation, are $\beta = 6a$ and $\gamma = 12a$. Other slip models are also represented by different values of β and γ. In fact, $\beta = 6a$ and $\gamma = 0$ gives the first order slip model of Burgdorfer,[1] $\beta = 6a$ and $\gamma = 6a$ gives the second order slip model

of Hsia and Domoto,[2] and finally $\gamma = 6a$ and $\gamma = 8/3$ gives the 1.5 order slip model of Mitsuya.[3]

III. 1-D THEORETICAL AND NUMERICAL SOLUTIONS NEAR A CONTACT POINT

We consider the 1-D problem of a moving surface with velocity U nearly contacted by a fixed asperity as shown in Fig. 2. To simplify the problem, we specify the dimensionless shape of the asperity as a parabola

$$H = \frac{AL^2}{h_0} X^2 + 1, \tag{7}$$

in which $A = 10^4\ 1/M$, $L = 0.5\mu M$. These parameters represent a typical size of the asperities in hard disk drives. The gas is assumed to be air at room temprature, under normal working conditions, $\mu = 1.85 \times 10^{-5} N \cdot S / M^2$, $p_a = 0.101 MPa$, $\lambda = 65 NM$, $U = 10 M/S$. h_0 is considered to be about 1 NM or less, approaching zero. For the one-dimensional case eq. (6) can be simplified and rearranged into

$$\frac{\partial}{\partial X}\left[\left(\frac{p_a h_0^2}{6\mu UL} PH^3 + \frac{\beta p_a \lambda h_0}{6\mu UL} H^2 + \frac{\gamma p_a \lambda^2}{6\mu UL}\frac{H}{P}\right)\frac{\partial P}{\partial X}\right] = \frac{\partial}{\partial X}(PH). \tag{8}$$

It is seen that the first two terms on the diffusion side are functions of the minimum spacing h_0, but the third term is not for models where γ is not equal to zero. As the spacing is reduced to contact or near contact, the first two terms can be dropped near the contact region, while the third term remains and provides the higher order slip effects. This regime is refered to as the higher order slip effect regime. Notice that the first and

second terms increase as the third and second powers of H, respectively. When H is increased somewhat, the second term dominates the third term and this is refered to as the first order slip effect regime, since its diffusion effect is dominated by the first order slip correction. As H increases further, the first term becomes dominant and the traditional continuum and non-slip regime is recovered.

For the problem under consideration here, the first two terms are much smaller than the third one even at the outer edge ($X = \pm 1$) where the largest H is found. As a result it is reasonable to keep only the third term. We define a new dimesionless parameter

$$\Gamma = \frac{\gamma p_a \lambda^2}{6\mu UL}. \tag{9}$$

Later we will show that the pressure distribution near the contact region depends only on this new parameter and one boundary condition at $X = 1$ or -1. Eq. (7) now assumes the simplified form

$$\frac{\partial}{\partial X}\left[\Gamma \frac{H}{P}\frac{\partial P}{\partial X}\right] = \frac{\partial}{\partial X}(PH), \tag{10}$$

which can be integrated once to give

$$\frac{dP}{dX} - \frac{1}{\Gamma}P^2 - \frac{C}{\Gamma H}P = 0, \tag{11}$$

where C is an integration constant. This is a Riccati equation which can be readily integrated again. After using the boundary condition at $X = -1$, we obtain

$$\frac{1}{P} = Exp\left(-\frac{C}{\Gamma}\int_{-1}^{X}\frac{1}{H}dx \right)\left[\frac{1}{P_L} - \frac{1}{\Gamma}\int_{-1}^{X} Exp\left(\frac{C}{\Gamma}\int_{-1}^{X}\frac{1}{H}dX \right)dX \right], \tag{12}$$

where C can be obtained from the boundary condition at $X = 1$. Since the right hand side of eq. (12) is quite complicated, a numerical root finding code similar to that of Ridders's method[10] is needed to find C. Using the geometry specified in eq. (7), we obtain from eq. (12)

$$\begin{aligned} P = Exp\left\{ \frac{C}{\Gamma L}\sqrt{\frac{h_0}{A}}\left[\mathrm{Atan}\left(\sqrt{\frac{A}{h_0}}L \right) + \mathrm{Atan}\left(\sqrt{\frac{A}{h_0}}LX \right) \right] \right\} \cdot \\ \left\{ \frac{1}{P_L} - \frac{1}{\Gamma}\int_{-1}^{X} Exp\left[\frac{C}{\Gamma L}\sqrt{\frac{h_0}{A}}\left[\mathrm{Atan}\left(\sqrt{\frac{A}{h_0}}L \right) + \mathrm{Atan}\left(\sqrt{\frac{A}{h_0}}LX \right) \right] \right] dX \right\}^{-1}. \end{aligned} \tag{13}$$

Then letting h_0 approach zero, we obtain the following closed form asymptotic solution with actual contact at $X = 0$ after using the boundary condition at $X = 1$,

$$P = \begin{cases} \dfrac{P_L\Gamma}{\Gamma - P_L(1+X)}, & -1 \le X < 0 \\ \dfrac{P_R\Gamma}{\Gamma + P_R(1-X)}, & 0 < X \le 1 \end{cases}. \tag{14}$$

When h_0 approaches zero in (13), C approaches to infinity so as to maintain $Ch_0^{0.5}$ constant to satisfy the boundary condition at $X = 1$.

An interesting property of the solution (14) is that a shock wave like discontinuity appears at the contact point. Before the contact point ($X < 0$), the solution depends only on the left boundary condition at $X = -1$. While the solution after the contact point ($X > 0$) depends only on the right boundary condition at $X = 1$. This is reasonable

physically, since the contact blocks communication between the two sides. Expression (14) clearly shows that the solution of the higher order slip correction model is bounded and integrable around the contact point.

To demonstrate that the present asymptotic analysis is valid we also numerically solved the full equation (8) with the boundary conditions $P_L = P_R = 1$, using a finite volume method for the convection and diffusion type equations similar to that in Patankar.[11] Figure 3 shows the pressure profiles predicted by the 1.5 order slip model ($\gamma = 8/3$) for different values of the minimum spacing. The analytical and numerical solutions are shown to be in good agreement in the limit of small spacing, which justifies discarding the higher order terms. As the minimum spacing is reduced, both the analytical and numerical solutions approach the asymptotic solution given by eq. (14). The solution clearly shows a boundary layer behavior near the minimum spacing point before the contact occurs. Furthermore, at contact the solution breaks into two separate branches at the contact point to form a shock wave type discontinuity. Figures 4 and 5 show similar curves of the second order slip model ($\gamma = 6a$) and our new slip model ($\gamma = 12a$).

From Figs 3-5, it is seen that the different models predict different pressures at the contact point, and the limit contact pressure at the upwind side is also quite different from that at the downwind side. The contact pressure at the upwind side is larger than the ambient pressure, due to the fact that although the contact brings the mean gas velocity to zero, the random motion of the gas molecules still produces a non-zero pressure at that point, the converging geometry compresses more molecules there than in the ambient region. As a result, a higher than ambient pressure is expected at the upwind contact

edge. A similar explanation can be used to explain why the contact pressure at the downwind side is lower than the ambient value. But neither value is zero, as was assumed by Huang and Bogy.[7] In their paper, the authors assumed that when the spacing is below the diameter of the gas molecules there are no gas molecules to provide pressure. As a result, they suggested setting the pressure to zero at each grid point where the spacing is below the gas molecule diameter as a numerical boundary condition in the numerical simulation to avoid the contact singularity. The above results suggest that their simple treatment may not be good enough to capture the complete physics at the contact point. Physically there must be a pressure jump from the region with a spacing larger than the molecule diameter to the region smaller than the molecule diameter. It is justified to set the pressure equal to zero in regions where gas molecules can not enter, but on the gas side edge, a value like that given by eq. (14) is needed to serve as the boundary condition. It is noted that Huang and Bogy's DSMC simulation also showed a subambient pressure in the downwind portion.[6]

Based on the above analysis, we now propose a way to supply the one needed boundary condition for contact geometries as shown in Fig. 6. For the left converging corner, one boundary condition at grid point $i = N$ is needed before the second order Reynolds equation can be solved numerically. If the geometry between grid points $i = N - 1$ and $i = N$ can be approximated by a papabola, then the contact pressure at the upwind side given by eq. (14) can be used at point N, while the length scale L is defined as $dX = X_N - X_{N-1}$. Result (14) also implies that L (the grid size) must be small enough to make Γ large enough so the denominator will not become zero when X is in the range –1 to 0. For geometries other than a parabola, similar analyses can be

conducted to derive a formula like eq. (14). Similar arguments hold for the right diverging corner problem.

For the first order slip model, $\gamma = 0$, and the third term on the left hand side of eq. (8) drops out. Then we only need to keep the second term to get

$$\frac{\partial}{\partial X}\left(\frac{\beta p_a \lambda h_0}{6\mu UL} H^2 \frac{\partial P}{\partial X}\right) = \frac{\partial}{\partial X}(PH). \tag{15}$$

After using the boundary condition at $X = -1$, we can integrate this simplified equation to obtain

$$P = Exp\left(\int_{-1}^{X} \frac{\Lambda}{\beta k_n} \frac{1}{H} dX\right) \cdot \left[1 + \frac{C\Lambda}{\beta k_n} \int_{-1}^{X} \frac{1}{H^2} EXP\left(-\int_{-1}^{X} \frac{\Lambda}{\beta k_n} \frac{1}{H} dX\right)\right]. \tag{16}$$

This equation has an unbounded singularity at the contact point.

For the FK model, near the contact point, the Reynolds equation can be written as

$$\frac{\partial}{\partial X}\left[-\frac{2\lambda P_a h_0}{\pi\mu UL} H^2 \log\left(\frac{\sqrt{\pi} h_0}{2\lambda} PH\right)\right] = \frac{\partial}{\partial X}(PH), \tag{17}$$

which can not be solved analytically.

Figures 7 and 8 show the numerical solutions of the first order slip model and the FK model as the minimum spacing is reduced, respectively. The two figures clearly demonstrate a trend toward an unbounded pressure singularity at the zero spacing when contact occurs. They also show the singularity is weaker for the FK model. At very small spacing the pressure profile is almost symetric around the contact point as opposed to the antisymmetric results in the bounded solutions and previous DSMC solutions of Huang and Bogy.[6] In fact this kind of behavier can be seen from eq. (15) and (17). When contact occurs, we can not use expression (7) to describe the geometry. Instead

$H = AL^2 X^2 / h_0$ can be used, where h_0 is taken to be a nonzero small characteristic spacing. $H -> 0$ as the contact point is approached. The diffusion term of the first order slip model scales like $O(H^2)$, while in the FK model it scales like $O(-H^2 \log H)$. When $H -> 0$, these terms are much smaller than the convection term, and as a result they can be ignored. The unbalanced convection produces a singular pressure C/H, where C is an integration constant. If the asperity geometry H is defined by a symmetric function about $X = 0$ (as for the previously studied parabola), the singular pressure profile is also symmetric about $X = 0$. Since $O(-H^2 \log H) >> O(H^2)$ as $H -> 0$, a weaker pressure singularity is expected for the FK model than for the first order slip model.

Since the convection term of the generalized Reynolds equation is of order $O(H)$ as $H -> 0$ the diffusion terms must also scale like $O(H)$ in order to balance the convection effect. Otherwise an $O(1/H)$ singularity is unavoidable. It was shown that for all the existing models only the 1.5 order slip model, the second order slip model and the new model derived here obey this kind of asymptotic behavior near the contact point. As a result, they are free of a contact pressure singularity. Other models which violate this condition, i.e. the first order slip model, the FK model and the continuum model, experience an unbounded contact singularity.

IV. 2-D NUMERICAL SOLUTION NEAR A CONTACT POINT

The two dimensional problem is much more difficult to treat analytically, so here we use numerical methods to demonstrate that the conclusions for the 1-D problem also

hold for the 2-D problem. The asperity is taken to be the axisymmetric one obtained by rotating the parabola (7). The domain is taken to be a square region $-1 \le X \le 1$ and $-1 \le Y \le 1$.

Since the performance of the higher order corrections and the new model are qualitatively the same, here we just use the second order slip model as an example. Figure 9 shows the pressure distributions along the $Y = 0$ center line. As the spacing is reduced, the pressure profile becomes steeper. When $h_0 = 1E-12M$, the curve is almost the same as that with contact. The contact curve does not have a shock wave discontinuity at the contact point, as did the 1-D problem, and the pressure distribution is much smoother than that of the 1-D problem with a lower peak pressure. This can be attributed to the cross diffusion effect introduced by the additional Y dimension. Figure 10 shows the pressure contour.

Figure 11 clearly demonstrates a trend of an unbounded singular pressure field for the first order slip model at the contact point as was seen in the 1-D problem. But its peak pressure is lower than that of the 1-D problem, which implies a weaker contact singularity here than in the 1-D problem. Figure 12 shows the corresponding pressure contours.

Figures 13 and 14 show the results for the FK model, and it is seen that they have the same quality as that of the first order slip model with a less steep distribution and lower peak pressure. They show contact singularities that appear to be weaker than that of the first order slip model.

V. DISCUSSION AND CONCLUSION

Following the approach of Anaya-Dufresne[8] to derive a slip boundary condition at the gas-solid interface through a momentum balance along the wall direction for the incompressible problem, we obtained the compressible counterpart, which is found to be the same as that of the incompressible case. The compressibility only introduces a higher order effect that can be ignored in the first order approximation. A new modified Reynolds equation for isothermal and compressible gas lubrication is then derived by using the new slip boundary condition. The resulting equation has a form similar to that of the second order and the 1.5 order slip models in the literature but with different coefficients that come from terms associated with the higher order slippage correction. However the higher order slippage correction terms of the second and 1.5 order slip models were derived from a purely mathematical point of view, i.e. they come from the second order Taylor series expension terms of the velocity field in the derivation of the slip boundary condition. In our derivation they come from the additional slippage introduced by the Poiseuille flow effect.

Theoretical and numerical simulations performed on a 1-D parabola contacting asperity show that there are no unbounded contact singularities for these higher order correction models. Instead, a shock wave like discontinuity appears at the contact point. When the asperity approaches contact, a boundary layer appears around the minimum spacing point. As the spacing is reduced, the pressure curve approaches continuously the one for contact. A new contact boundary condition for the Reynolds equation at the converging or diverging corner is proposed, based on the asymptotic analysis, which can be used as the numerical boundary condition at the contact edge in the numerical simulation if locally the geometry near the contact point can be approximated by a

parabola. For the first order slip model and the FK model, we analytically and numerically showed that a symmetric contact singularity of $O(1/H)$ appears at the contact point as $H->0$. A general conclusion can be drawn, that for any modified Reynolds equation to be free of a contact singularity, it must have diffusion terms that go to zero no faster than the convection terms near the contact point as the minimun spacing is reduced to zero.

ACKNOWLEDGEMENTS

This work was supported by the Computer Mechanics Laboratory at the University of California at Berkeley.

[1] A. Burgdorfer, “The influence of the molecular mean free path on the performance of hydrodynamic gas lubricated bearing,” ASME J. of Basic Engineering, **81**, 94 (1959).

[2] Y. T. Hsia and G. A. Domoto, “An experimental investigation of molecular rarefaction effects in gas lubricated bearings at ultra-low clearances,” ASME J. of Lubrication Technology, **105**, 120 (1983).

[3] Y. Mitsuya, “Modified Reynolds equation for ultra-thin film gas lubrication using 1.5-order slip-flow model and considering surface accommodation coefficient,” ASME J. of Tribology, **115**, 289 (1993).

[4] S. Fukui and R. Kaneko, “A database for interpolation of Poiseuille flow rates for high Knudsen number lubrication problems,” ASME J. of Tribology, **110**, 335 (1988).

[5] M. Anaya-Dufresne and G. B. Sinclair, “On the breakdown under contact conditions of Reynolds equation for gas lubricated bearings,” ASME J. of Tribology, **119**, 71 (1997).

[6] W. Huang and D. B. Bogy, “An investigation of a slider air bearing with a asperity contact by a three dimensional direct simulation Monte Carlo method,” IEEE Trans. on Magnetics, **34**, 1810 (1998).

[7] W. Huang, M. Honchi and D. B. Bogy, "An asperity contact model for the slider air bearing," ASME J. Tribology, **122**, 436, (2000).

[8] M. Anaya-Dufresne, “On the development of a Reynolds equation for air bearings with contact,” Doctoral dissertation, Department of Mechanical Engineering, Carnegie Mellon University, Pittsburgh, PA (1996).

[9] E. H. Kennard, *Kinetic Theory of Gases*, Mcgraw-Hill Book Co., New York (1938).

[10] W. H. Press, S. A. Teukolsky, W. T. Vetterling and B. P. Flannery, *Numerical Recipes in Fortran 77*, Cambridge University Press (1992).

[11] S. V. Patankar, *Numerical Heat Transfer and Fluid Flow*, McGraw-Hill, New York (1980).

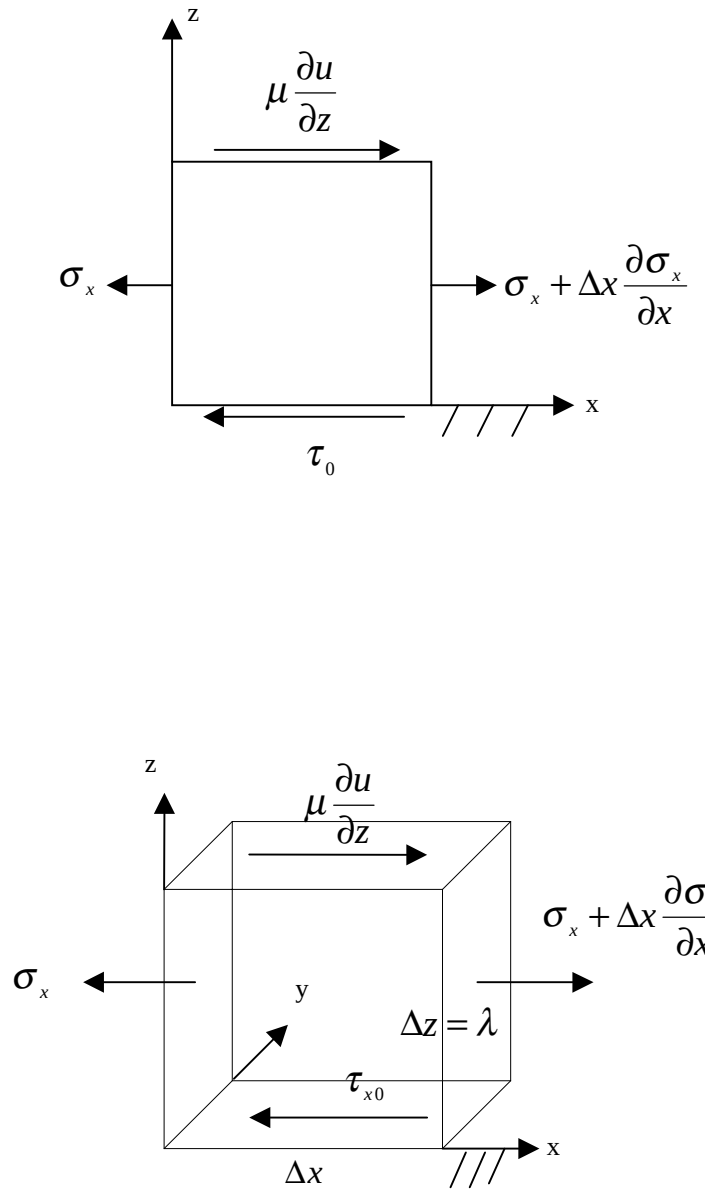

FIG. 1. The control volume for momentum balance in the x direction with higer order stress contributions ignored under gas lubrication condition.

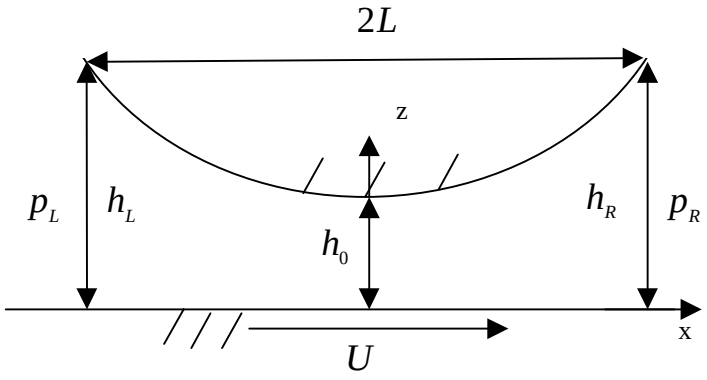

FIG.2. The assumed geometry of the contacting asperity.

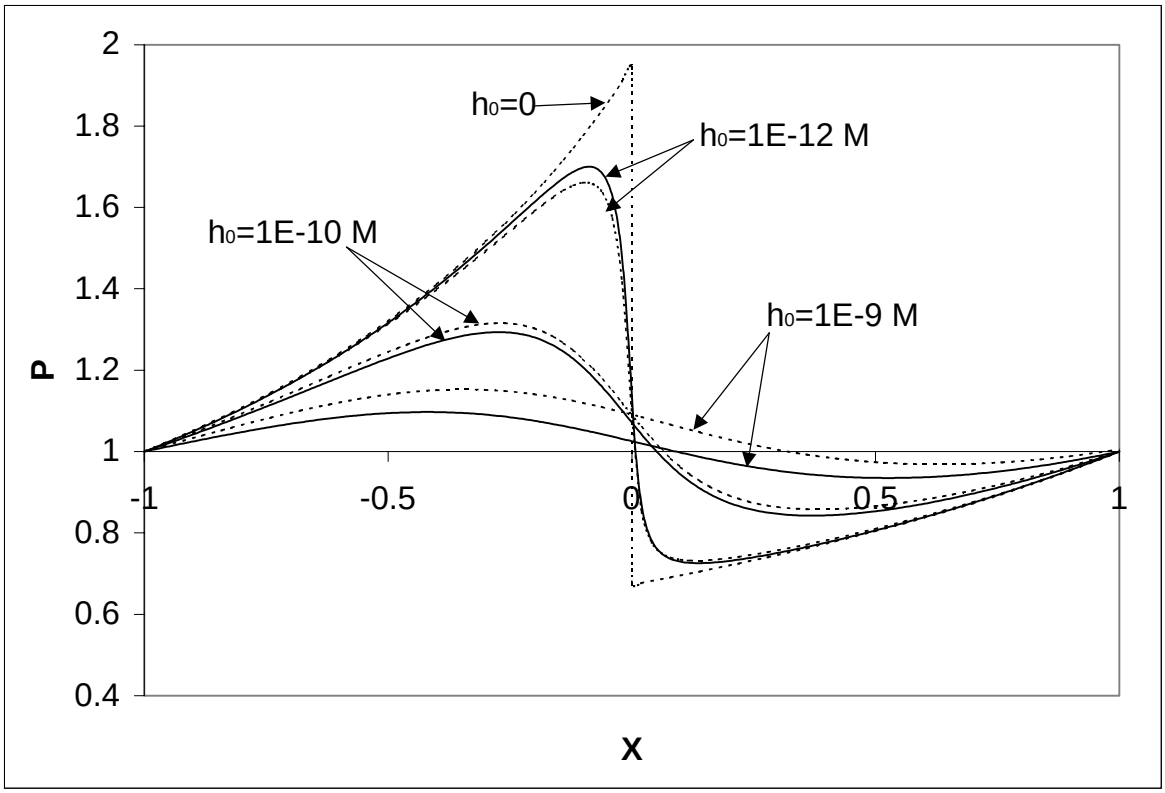

FIG. 3. The pressure profiles predicted by the 1.5 order slip model ($\gamma = 8/3$) for different minimum spacing h_0; Solid line: numerical solution of full eq. (8); dashed line: analytical solution given by eq. (13) and the asymptotic curve of eq. (14) (when $h_0 = 0$).

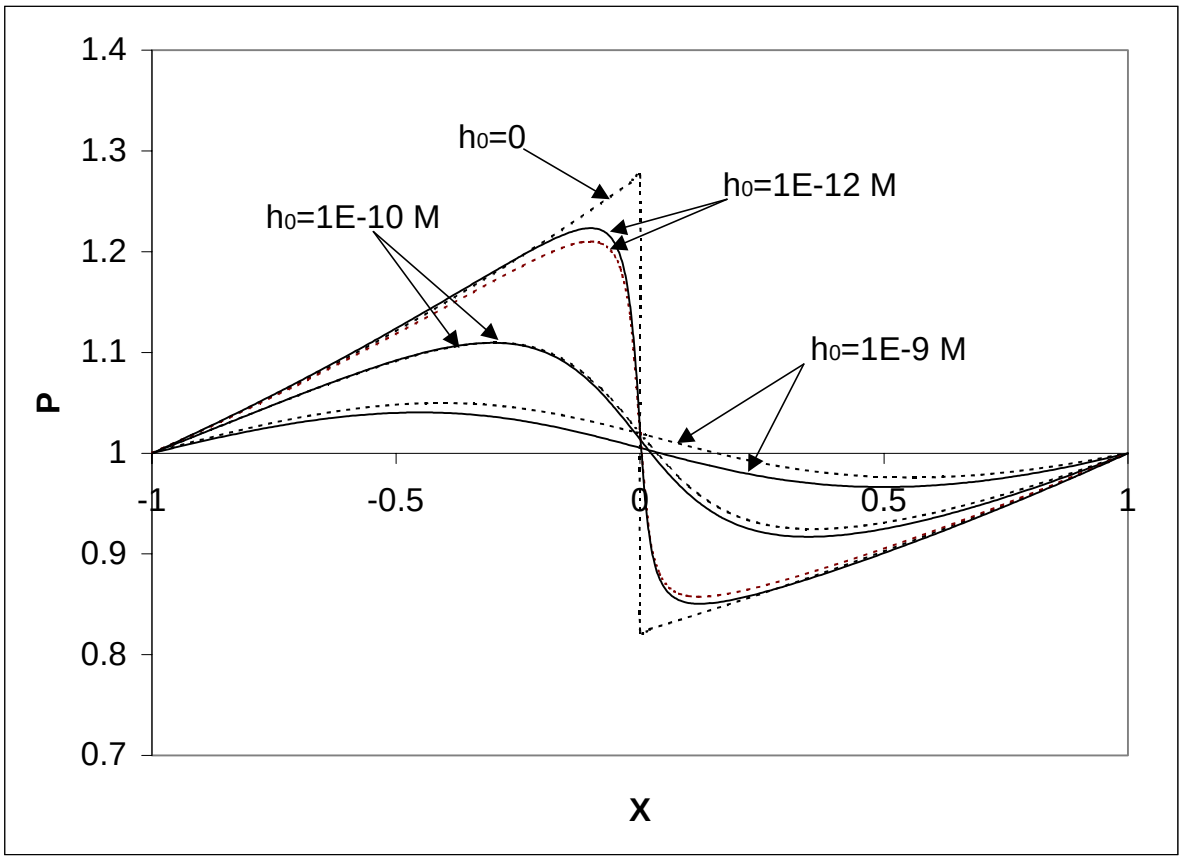

FIG. 4. The pressure profiles predicted by the second order slip model ($\gamma = 6a$) for different minimum spacing h_0; Solid line: numerical solution of full eq. (8); dashed line: analytical solution given by eq. (13) and the asymptotic curve of eq. (14) (when $h_0 = 0$).

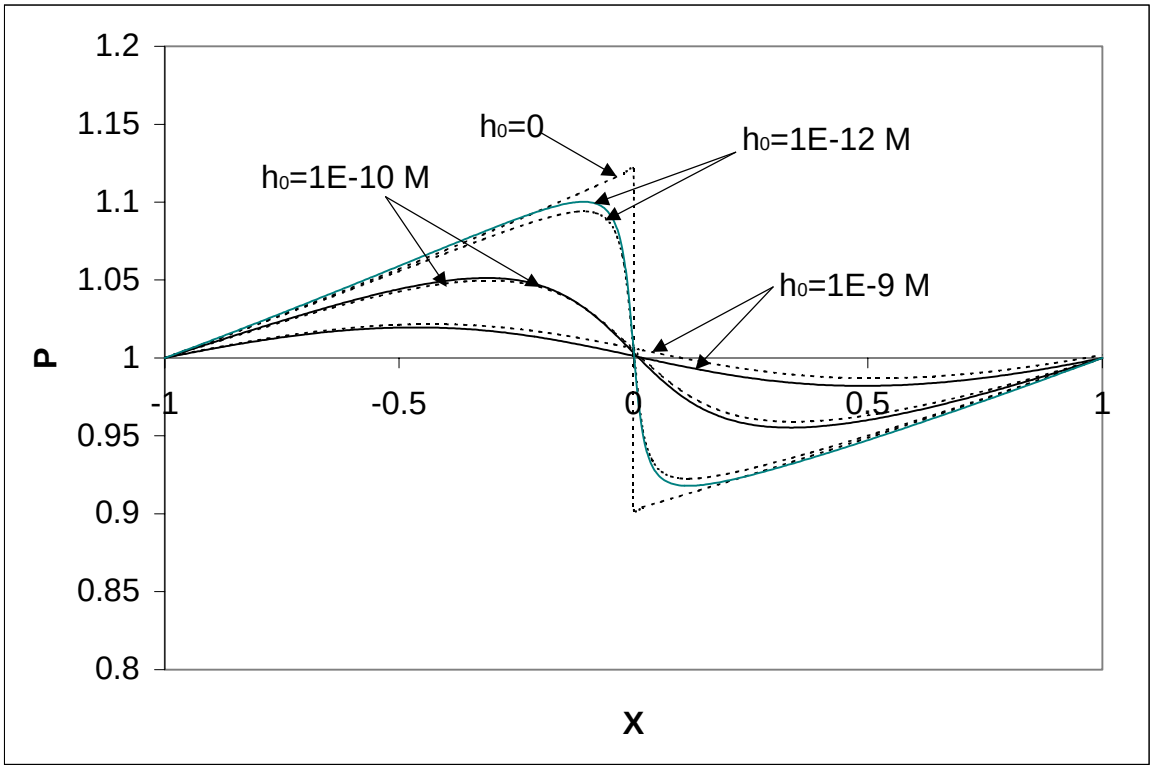

FIG. 5. The pressure profiles predicted by the new order slip model ($\gamma = 12a$) for different minimum spacing h_0; Solid line: numerical solution of full eq. (8); dashed line: analytical solution given by eq. (13) and the asymptotic curve of eq. (14) (when $h_0 = 0$).

FIG. 6. The converging corner and the diverging corner around a contact area.

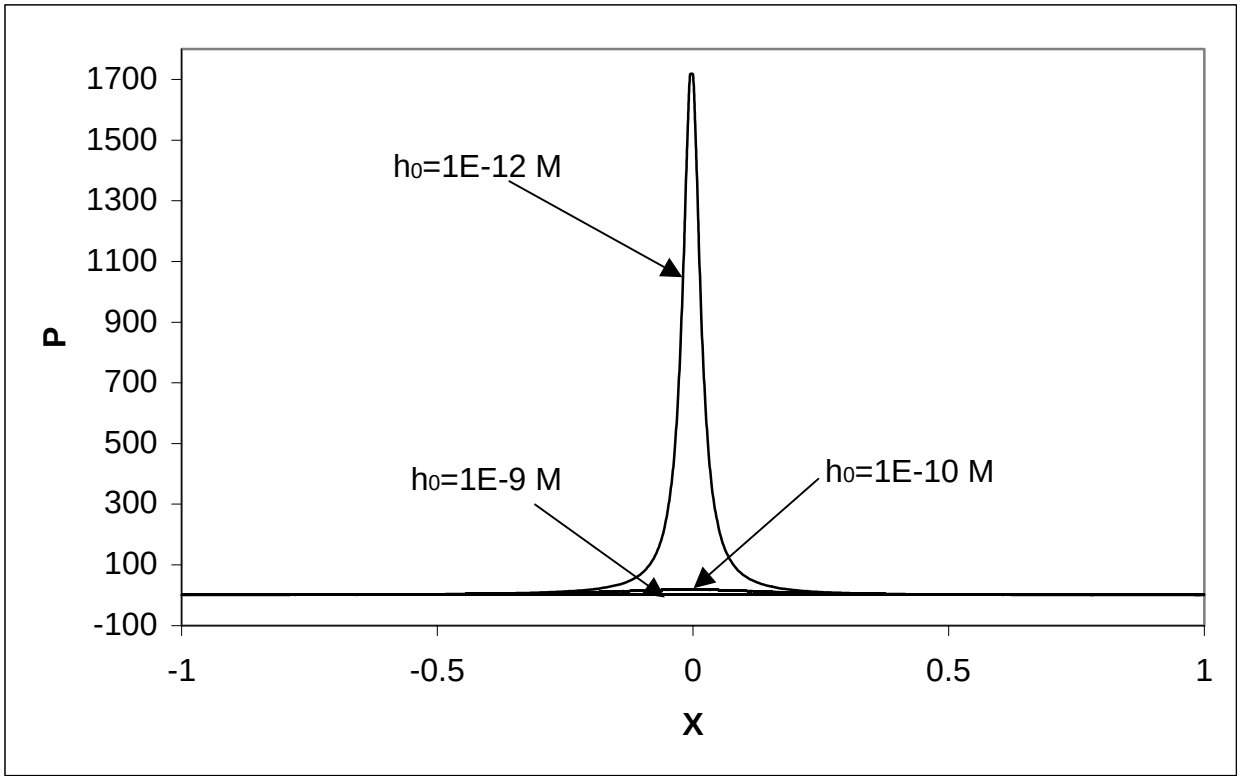

FIG. 7. The pressure profiles predicted by the first order slip model for different minimum spacings.

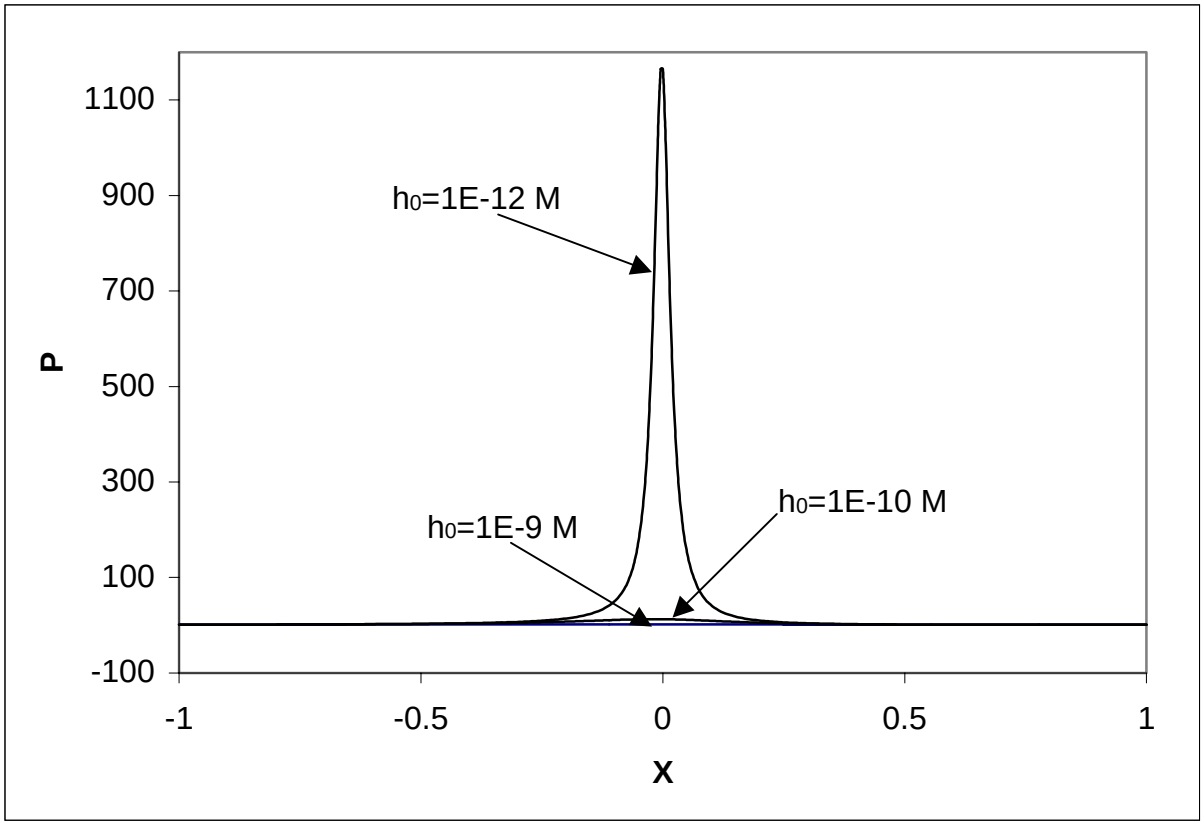

FIG. 8. The pressure profiles predicted by the FK model for different minimum spacings.

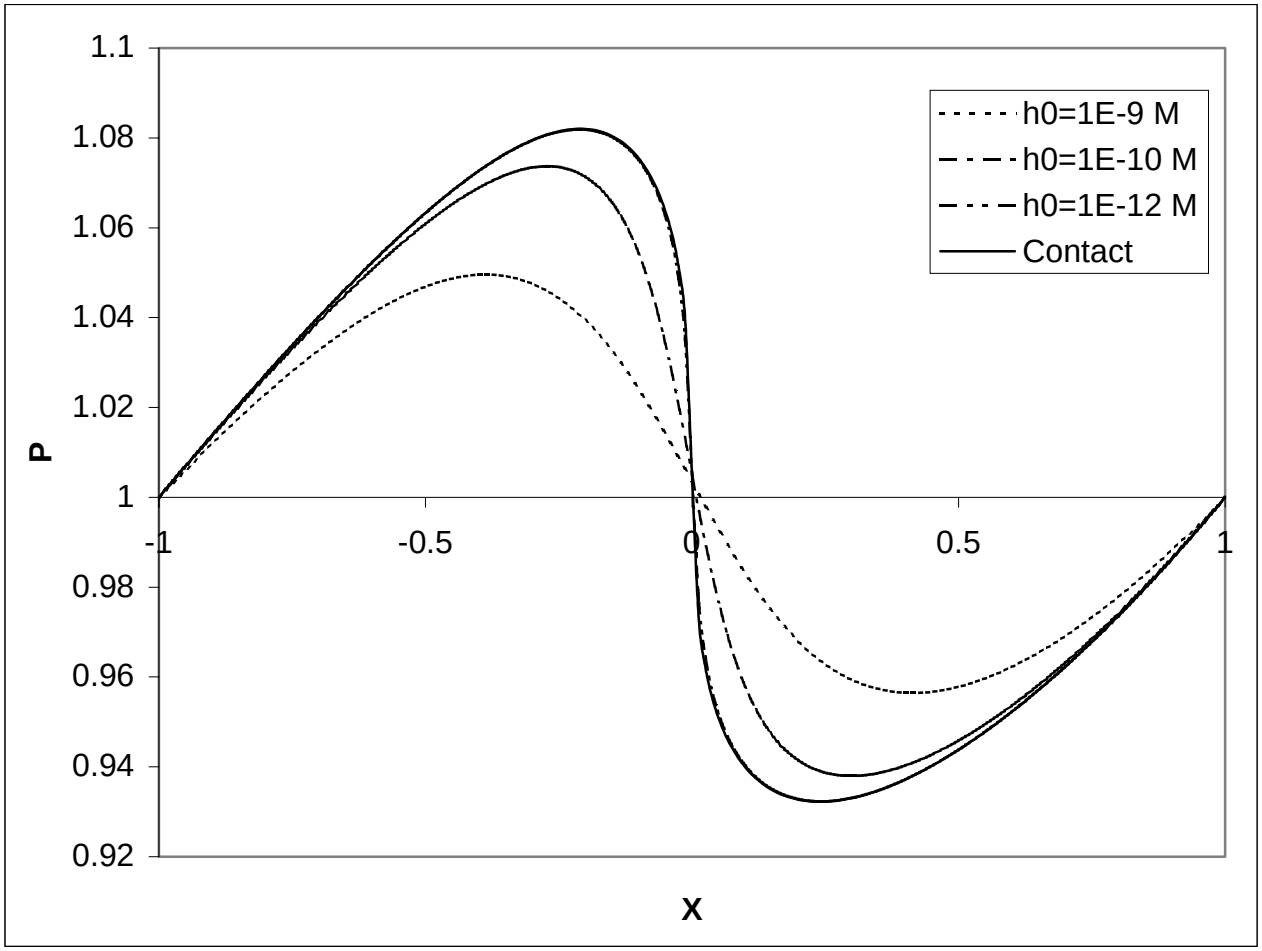

FIG. 9. The pressure profiles along the center line $Y = 0$ for the two dimensional problem as predicted by the second order slip model for different minimum spacings.

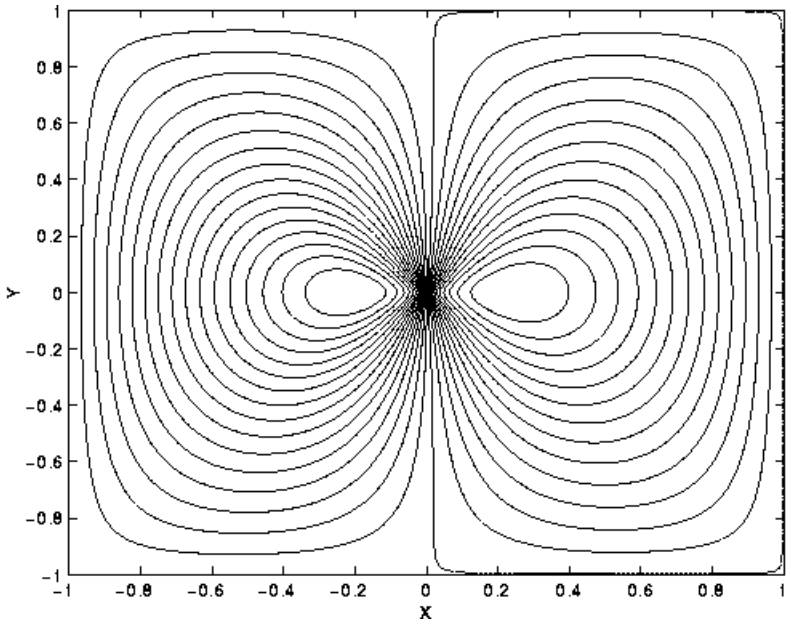

FIG. 10. The pressure contours for the two dimensional problem predicted by the second order slip model with contact.

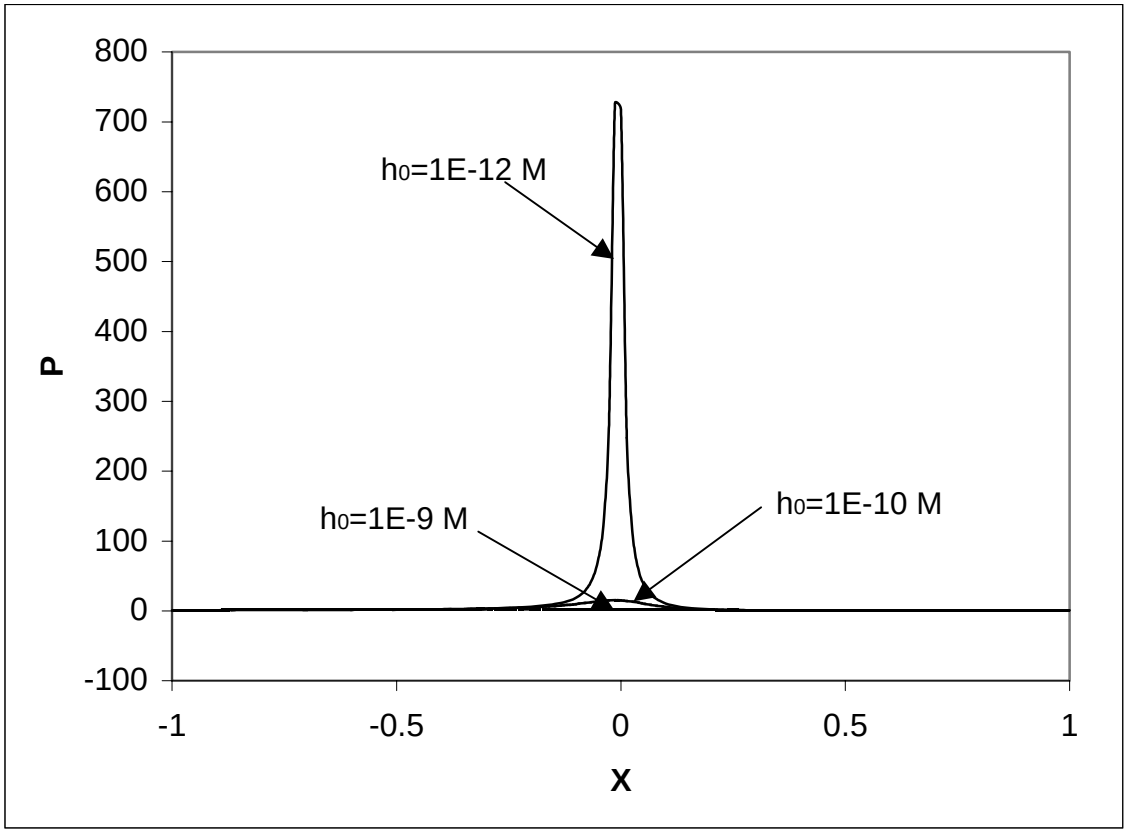

FIG. 11. The pressure profiles at the center line $Y = 0$ for the two dimensional problem predicted by the first order slip model for different minimum spacings.

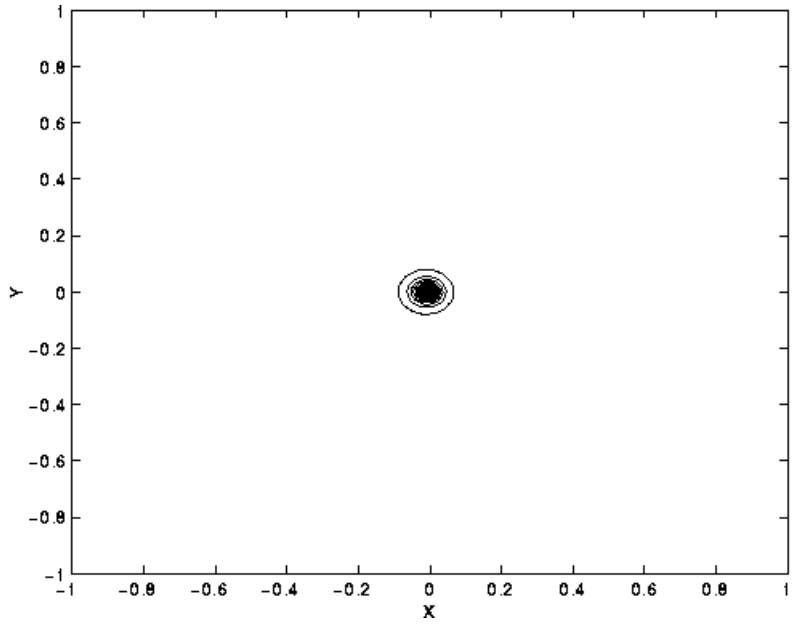

FIG. 12. The pressure contours for the two dimensional problem as predicted by the first order slip model with $h_0 = 1E-12\ M$.

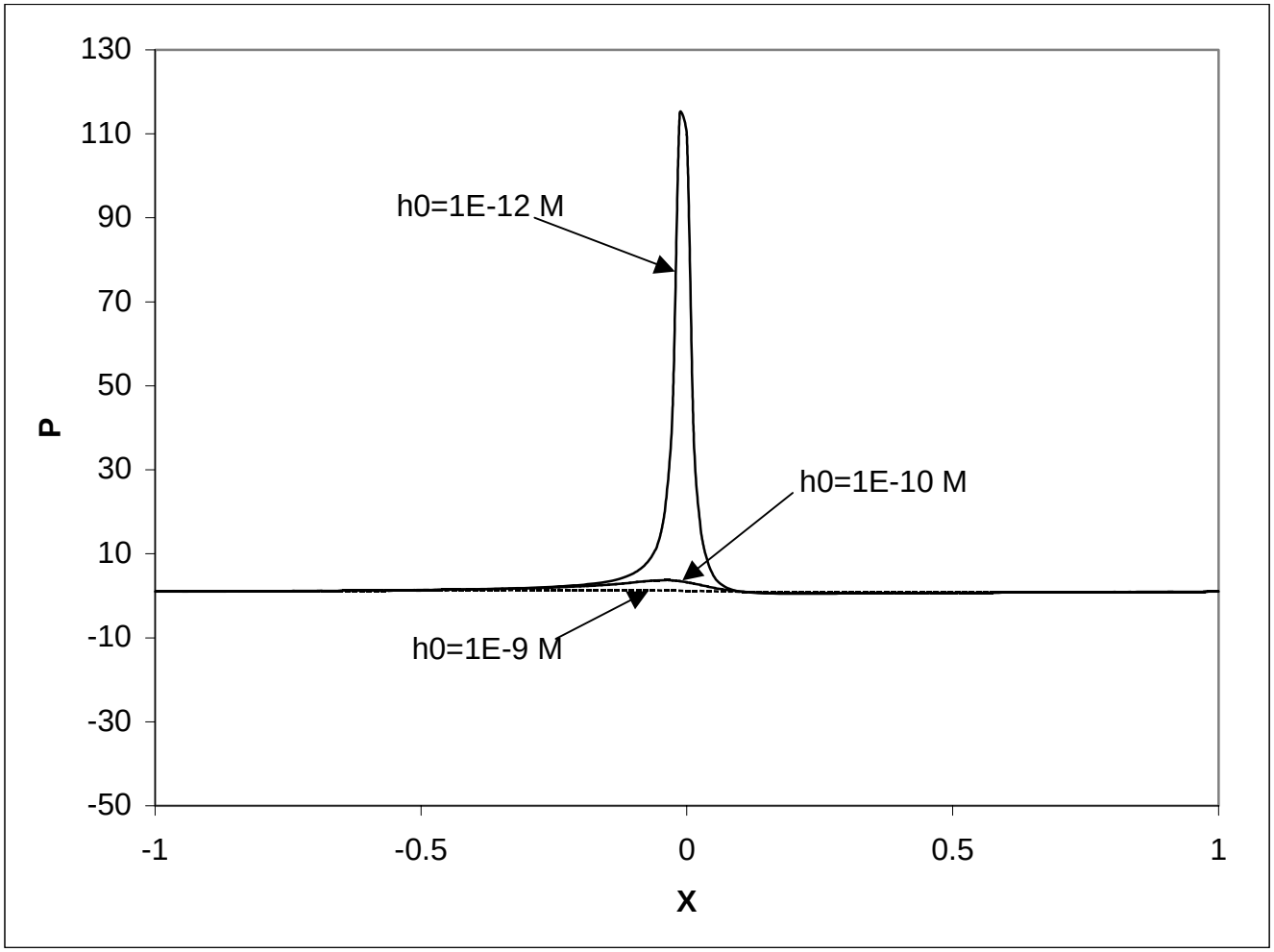

FIG. 13. The pressure profiles along the center line $Y = 0$ for the two dimensional problem as predicted by the FK model for different minimum spacings.

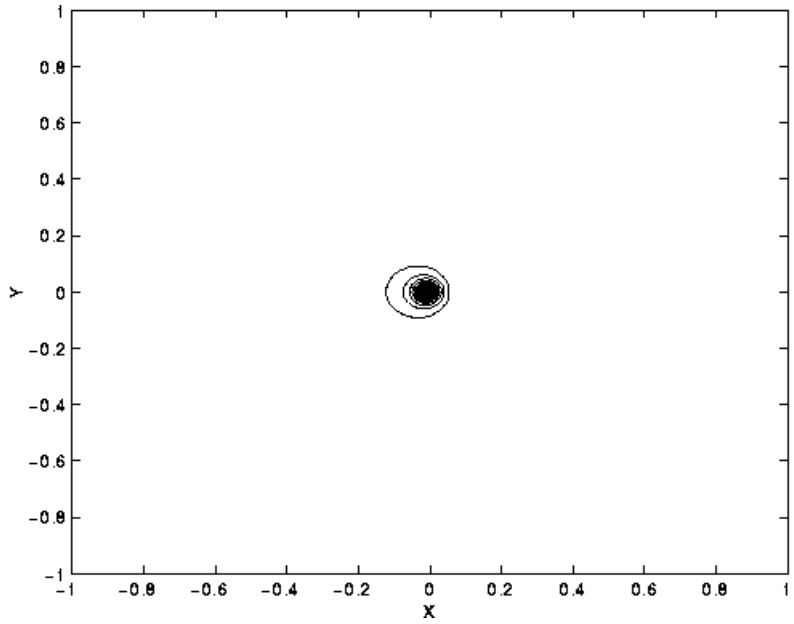

FIG. 14. The pressure contours for the two dimensional problem as predicted by the FK model with $h_0 = 1E-12\ M$.